One-Electron Reduction and Oxidation Studies of the Radiation Sensitizer Gadolinium(III) Texaphyrin (PCI-0120) and Other Water Soluble Metallotexaphyrins

Jonathan L. Sessler,*,† Nicolai A. Tvermoes,† Dirk M. Guldi,‡ Tarak D. Mody,§ and William E. Allen†

Department of Chemistry and Biochemistry, University of Texas at Austin, Austin, Texas 78712, Radiation Laboratory, University of Notre Dame, Notre Dame, Indiana 46556, and Pharmacyclics, Inc., 995 East Arques Avenue, Sunnyvale, California 94086

Received: September 24, 1998; In Final Form: December 24, 1998

The radiation sensitizer gadolinium(III) texaphyrin **2** (XYTRIN; PCI-0120; Gd−Tex^{2+}) and several other water soluble metallotexaphyrin complexes were prepared and studied using pulse radiolysis. All of the metallotexaphyrins were found to react with solvated electrons and hydroxyl radicals, yielding the corresponding one-electron reduced and oxidized metallotexaphyrins, respectively. The rates of the reduction processes range from 3.7×10^{10} to 6.8×10^{10} M^{-1} s^{-1} (±10%), while those involving oxidation range from 2.5×10^{9} to 7.4×10^{9} M^{-1} s^{-1} (±10%). The spectral characteristics of the transformed metallotexaphyrins produced by these reactions, e.g., a broad absorption band with a λ_{max} centered around 830 nm, are consistent with ligand-centered redox processes. Reaction of the metallotexaphyrins with solvated electrons affords species which exhibit metal dependent behavior. In the absence of hydroxyl radicals, the decay of the reduced metallotexaphyrins produced by reaction with electrons involves an initial protonation event followed by either a dimerization process or a disproportionation step. These latter transformations are followed by a second protonation event.

Introduction

An estimated 1.4 million American patients were diagnosed with cancer for the first time in 1997.[1] Of these, more than 60% will receive some kind of radiation treatment.[2,3] Unfortunately, the side effects associated with radiation treatment can be severe, and a large number of patients treated in this manner will not be cured of their disease. It is believed that the often-limited therapeutic gain of X-ray radiation therapy (XRT) arises from the presence of hypoxic cells within the tumor.[4] Hypoxic cells are typically 2.5−3 times less sensitive to radiation than oxygenated cells.[5] Not surprisingly, therefore, several different approaches to overcoming the radioresistance of hypoxic cells, e.g., radiation fractionation, administration of hyperbaric oxygen, etc.,[6−8] have been pursued.

A different approach involves using externally administered agents, so-called radiation sensitizers, to enhance the radiosensitivity of the tumor chemically.[9−11] The halogenated pyrimidines[11−13] and the nitroimidazoles[14−30] are among the most extensively studied of the various small molecule radiation sensitizers tested to date.[7,9,10] However, neither has lived up to initial expectations. For instance, the radiation-sensitizing efficacy of the halogenated pyrimidines has been shown to be dependent upon the efficiency with which they are incorporated into DNA.[31,32] This, in turn, has limited their clinical utility, in part because many cancers have a low fraction of cells in the so-called S phase (i.e., actively replicating DNA).[33] For the nitroimidazoles, both central and peripheral neurotoxicity and low levels of into-tumor localization have served to restrict their utility as radiation sensitizers.[34] Thus, the search for improved radiation sensitizers continues. Ideally, such improved sensitizing systems should demonstrate low inherent toxicity, should operate via a mechanism that does not require oxygen, and should not require incorporation into DNA.

Currently, despite a great deal of effort and a number of promising leads, not a single agent has been approved as a radiation sensitizer in the United States. In fact, to the best of our knowledge, the gadolinium(III) diacetate complex of the pentadentate macrocycle texaphyrin,[35−44] (**2**; XYTRIN; PCI-0120; Gd−Tex^{2+}),[45] is the only porphyrin or porphyrin-like molecule undergoing XRT-related human clinical trials in either the United States or Europe.[46,47] This experimental drug is currently undergoing a Phase III clinical trial for brain metastases.

There are two critical features of the metallotexaphyrins that led to the consideration that they could function as radiation sensitizers. First, this class of molecules, like the porphyrins, is known to localize with high selectivity in cancerous tissues.[48] Second, the metallotexaphyrins are known to contain a low-lying LUMO; in comparison to porphyrins and most other endogenous species, they are thus very easy to reduce ($E_{1/2} \approx$ 0.08 V vs NHE; aqueous, pH 7).[43,46,47] Taken together, these two facts led to the proposal that the water-soluble, MRI-detectable gadolinium(III) texaphyrin could function as a good radiation sensitizer.[43]

In this paper we report the results of pulse radiolysis experiments carried out with **2** and several analogous lanthanide (**3**−**7**) and nonlanthanide (**8**−**10**) metallotexaphyrins, focusing on the selective generation of their one-electron reduced and oxidized states. These studies, predicated on the use of pulse radiolysis, have allowed us to probe the effect of metal size and spin upon metallotexaphyrin reactivity and to assess the stability of the resulting redox products. Such studies were

† University of Texas.
‡ University of Notre Dame.
§ Pharmacyclics, Inc.

10.1021/jp9838588 CCC: $18.00
Published on Web 02/03/1999

deemed of particular importance in view of the recent finding that the analogous lutetium texaphyrin complex (**7**; LUTRIN; PCI-0123; Lu−Tex^{2+}) is not appreciably active as a radiation sensitizer in vivo under the same conditions where Gd−Tex^{2+} (**2**) is found to be effective.[49]

Experimental Section

Electrochemical measurements were performed using a Bioanalytic Systems Inc. (BAS) CV-50W Version 2 MF 9093 voltammetric analyzer. Solutions of either 0.1 M tetrabutylammonium perchlorate in DMF or 0.1 tetrabutylammonium tetrafluoroborate in 2-propanol were used in these studies. These were purged with argon prior to each measurement. The concentration of M−Tex^{2+} was approximately 0.9 mM. The working electrode was a platinum disk of 1.6 mm diameter, a platinum wire was used as the auxiliary electrode, and the reference electrode consisted of an Ag/AgCl couple.

Pulse radiolysis experiments were performed utilizing 50 ns pulses of 8 MeV electrons from a Model TB-8/16-1S electron linear accelerator (Notre Dame Radiation Laboratory). A complete description of the instrumentation and techniques has been reported previously.[50,51] The dose per pulse was determined by potassium thiocyanate dosimetry to be approximately 14 Gy, yielding total radical concentrations between 2 and 8 μM. Sample solutions contained ca. 15 or 100 μM M−Tex^{2+} in 2.0 mM aqueous phosphate buffer. Reducing and oxidizing conditions were obtained by addition of 2 vol % *tert*-butyl alcohol/purging with N_2, or by purging with oxygen free N_2O, respectively. Differential absorption (ΔOD) spectra of both the reduced and oxidized species from 500 to 900 nm were measured point-by-point without correcting for the consumption of the parent texaphyrin. A confirming experiment under oxidizing conditions was performed using a N_2O-purged aqueous NaCl (10 mM) solution at pH = 3.2 with texaphyrin concentrations ranging from 0 to 4.1 μM. All experiments were conducted at room temperature (21 ± 2 °C).

Synthetic Experimental Section

General Information. Electronic spectra were recorded on a Hitachi-U3000 spectrophotometer in methanol or 96% methanol/4% acetic acid (v/v). All low- and high-resolution and electrospray mass spectra were obtained from the University of California Mass Spectrometry Laboratory, Berkeley, CA. All elemental analyses were performed by Schwarzkopf Microanalytical Laboratory, Woodside, NY.

Materials. All solvents were of reagent grade quality and purchased commercially. Metal salts were purchased from Alfa AESAR (Ward Hill, MA). LZY-54 zeolite was purchased from UOP (Des Plaines, IL). Ambersep 900 (OH) anion-exchange resin was purchased from Rohm and Haas Co. (Philadelphia, PA). Thin-layer chromatography (TLC) of the metallotexaphyrin complexes was carried out using a 4:1:2 v/v/v mixture of 1-butanol, acetic acid, and water, respectively, on Whatman K6F silica gel plates. Merck-Type 60 (230−400 mesh) silica gel was used for column chromatography.

Synthesis. General Procedure for the Synthesis of Water-Soluble Texaphyrin Complexes of 4,5-Diethyl-10,23-dimethyl-9,24-bis(3-hydroxypropyl)-16,17-bis[2-[2-(2-methoxyethoxy)ethoxy]ethoxy]pentaazapentacyclo[20.2.1.13,6.18,11.014,19]heptacosa-1,3,5,7,9,11(27),12,14,16,18,20,22(25),23-tridecaene (1). One equivalent of the hydrochloride salt of the macrocyclic ligand **11**,[42] 1.0−1.5 equiv of the relevant $M(OAc)_{n+1}\cdot xH_2O$ salt, and 10 equiv of triethylamine were mixed together in methanol (25−200 mL/g of macrocycle), and the mixture was heated to reflux while left exposed to air.[42] During the course of the reaction, air was periodically bubbled directly into the reaction vessel using a dispersion tube. The progress of the reaction was monitored by UV/vis spectroscopy and TLC. After the reaction was deemed complete, the deep green solution was cooled to room temperature, filtered through a pad of Celite, and stripped of solvent under reduced pressure. The resulting complex was then purified using the following procedure: (1) acetone trituration, (2) removal of free metal by zeolite extraction, (3) counterion exchange by acetic acid washed Ambersep 900 resin, and (4) crystallization using mixed solvent systems ethanol/*n*-heptane (1:3 v/v) or ethanol/isopropyl alcohol (95:5 v/v), as described further below.

The crude metallotexaphyrin product, a dark green solid, was suspended in acetone (25 mL/g of starting nonaromatic macrocycle), stirred for 30 min at room temperature, and then filtered to wash away the red/brown impurities (incomplete oxidation products and excess triethylamine). The resulting green solid was dried in vacuo. A weighed quantity of this material was then dissolved into MeOH using 35 mL of solvent/g of crude metallotexaphyrin complex, and the solution was stirred for ~30 min and then filtered through Celite into a 1 L Erlenmeyer flask. Deionized water (3.5 mL/g of crude complex) was added to the flask along with LZY-54 zeolite that had been prewashed with acetic acid (5 g zeolite/g of crude complex). The resulting mixture was agitated or shaken for 1−3 h and then filtered through Celite to remove the zeolite. This latter procedure, which constitutes a free metal extraction, was performed twice in order to ensure that the residual levels of free metal were low (i.e., <0.2 wt %). Once this process was complete, the filtrate was loaded onto a column (30 cm length × 2.5 cm diameter for a reaction run on the 1−5 g scale) of Ambersep 900 anion-exchange resin (pretreated so as to be in the acetate form) and eluted with MeOH. The eluent containing the bis-acetate complex was collected, concentrated to dryness under reduced pressure, and recrystallized from either anhydrous ethanol/*n*-heptane (1:3 v/v) at 60 °C or boiling ethanol/isopropyl alcohol (95:5 v/v). The final product was collected by filtration on a fritted glass funnel and dried in vacuo at 40−45 °C for 24−48 h.

HPLC Analysis. The purity of all new metallotexaphyrins employed in this study (e.g., **2**−**10**) was checked using HPLC analysis (i.e., >90% relative purity). The system employed was from Waters/Millipore and was composed of a 600E Systems Controller with a 510 pump, a 717 Autosampler, and a 996 photodiode array detector. The detector monitored the elution profile from 250 to 800 nm. A C_{18} reversed-phase column was employed (Inertsil ODS2, 5 m particle, from GL Science, Japan; packed by Metachem; the final column dimensions were 150 mm × 4.6 mm). All mobile phase media were HPLC grade and obtained from Baxter. The mobile phase consisted of a 100 mM ammonium acetate buffer (pH adjusted to 4.3 with glacial acetic acid) and acetonitrile. The column was first eluted with 72% 100 mM ammonium acetate buffer and 28% acetonitrile for 28 min. A linear gradient was then applied over the next 10 min to reach 20% 100 mM ammonium acetate buffer and 80% acetonitrile. The flow rate was 1.5 mL/min with the column temperature set at 40 °C.

Gadolinium(III) Complex 2. The nonaromatic macrocycle **11** (31 g, 33.9 mmol), $Gd(OAc)_3\cdot 4H_2O$ (15.8 g, 38.9 mmol) and triethylamine (34.3 g, 339 mmol) were mixed together in methanol (1 L), and the mixture was heated to reflux in the air. Using the general procedure described above, the reaction was deemed complete after 7 h. After workup and recrystallization

from ethanol/*n*-heptane as described above, 27.3 g (70%) of **2** was obtained in the form of a dark green microcrystalline solid. UV/vis [(λ_{max}, nm, in MeOH) (log ϵ)]: 350 (4.33), 414 (4.67), 473 (5.06), 739 (4.59). FAB MS, [M − 2OAc$^-$]$^+$: *m*/*z* 1030. HRMS, [M − 2OAc$^-$]$^+$: *m*/*z* 1027.4016 (calcd for [$C_{48}H_{66}$-$^{155}GdN_5O_{10}$]$^{2+}$, 1027.4036). Anal. Calcd for [$C_{48}H_{66}GdN_5O_{10}$]-$(OAc)_2(H_2O)_{1/2}$: C, 53.96; H, 6.36; N, 6.05; Gd, 13.59. Found: C, 53.96; H, 6.34; N, 6.11; Gd, 13.68.

Europium(III) Complex 3. The hydrochloride salt of macrocycle **11** (1.5 g, 1.64 mmol), $Eu(OAc)_3 \cdot 4H_2O$ (0.72 g, 1.80 mmol) and triethylamine (1.66 g, 16.4 mmol) were mixed together in methanol (100 mL) and heated to reflux in the air. Using the general procedure described above, the reaction was deemed complete after 5 h. After workup and recrystallization from ethanol/*n*-heptane as described above, 1 g (53%) of **3** was obtained in the form of a dark green microcrystalline solid. UV/vis [(λ_{max}, nm for Soret-type and Q-type absorption bands, in 96% MeOH/4% acetic acid) (log ϵ)]: 474 nm (5.08), 740 nm (4.61). FAB MS, [M − 2OAc$^-$]$^+$: *m*/*z* 1025. HRMS, [M − 2OAc$^-$]$^+$: *m*/*z* 1023.3997 (calcd for [$C_{48}H_{66}EuN_5O_{10}$]$^{2+}$, 1023.4008). Anal. Calcd for [$C_{48}H_{66}EuN_5O_{10}$]$(OAc)_2(H_2O)_{1/2}$: C, 54.21; H, 6.39; N, 6.08; Eu, 13.19. Found: C, 54.03; H, 6.55; N, 6.15; Eu, 13.45.

Dysprosium(III) Complex 4. The hydrochloride salt of macrocycle **11** (4.0 g, 4.38 mmol), $Dy(OAc)_3 \cdot 4H_2O$ (2.25 g, 5.47 mmol), and triethylamine (4.4 g, 43.8 mmol) were mixed together in methanol (100 mL), and the mixture was heated to reflux in the air. Using the general procedure described above, the reaction was deemed complete after 3.5 h. After workup and recrystallization from ethanol/*n*-heptane as described above, 3.2 g (63%) of **4** was obtained in the form of a dark green microcrystalline solid. UV/vis [(λ_{max}, nm for Soret-type and Q-type absorption bands, in 96% MeOH/4% acetic acid) (log ϵ)]: 474 nm (5.08), 736 nm (4.61) FAB MS, [M − 2OAc$^-$ + H]$^+$: *m*/*z* 1037. HRMS, [M − 2OAc$^-$]$^+$: *m*/*z* 1036.4110 (calcd for [$C_{48}H_{66}DyN_5O_{10}$]$^{2+}$, 1036.4102). Anal. Calcd for [$C_{48}H_{66}$-DyN_5O_{10}]$(OAc)_2(H_2O)$: C, 53.31; H, 6.37; N, 5.98; Dy, 14.09. Found: C, 53.16; H, 6.23; N, 5.93; Dy, 13.85.

Thulium(III) Complex 5. The hydrochloride salt of macrocycle **11** (2.0 g, 2.2 mmol), $Tm(OAc)_3 \cdot 4H_2O$ (1.2 g, 2.9 mmol) and triethylamine (2.3 g, 23 mmol) were mixed together in methanol (400 mL), and the mixture heated to reflux in the air. Using the general procedure described above, the reaction was deemed complete after 7 h. After workup and recrystallization from ethanol/isopropyl alcohol as described above, 1.8 g (71%) of **5** was obtained in the form of a dark green microcrystalline solid. UV/vis [(λ_{max}, nm for Soret-type and Q-type absorption bands, in 96% MeOH/4% acetic acid) (log ϵ)]: 475 nm (5.12), 733 nm (4.65). FAB MS, [M − 2OAc$^-$]$^+$: *m*/*z* 1042. HRMS, [M − 2OAc$^-$]$^+$: *m*/*z* 1041.4170 (calcd for [$C_{48}H_{66}TmN_5O_{10}$]$^{2+}$, 1041.4152). Anal. Calcd for [$C_{48}H_{66}TmN_5O_{10}$]$(OAc)_2(H_2O)_{1/2}$: C, 53.42; H, 6.29; N, 5.99; Tm, 14.45. Found: C, 53.44; H, 6.26; N, 5.76; Tm, 14.70.

Ytterbium(III) Complex 6. The hydrochloride salt of macrocycle **11** (2.1 g, 2.3 mmol), $Yb(OAc)_3 \cdot xH_2O$ (1.2 g, 2.9 mmol) and triethylamine (2.3 g, 23 mmol) were mixed together in methanol (400 mL), and the mixture was heated to reflux in the air. Using the general procedure described above, the reaction was deemed complete after 18 h. After workup and recrystallization from ethanol/isopropyl alcohol as described above, 1.85 g (69%) of **6** was obtained in the form of a dark green microcrystalline solid. UV/vis [(λ_{max}, nm for Soret-type and Q-type absorption bands, in 96% MeOH/4% acetic acid) (log ϵ)]: 475 nm (5.11), 732 nm (4.65). FAB MS, [M − 2OAc$^-$]$^+$: *m*/*z* 1046; HRMS, [M − 2OAc$^-$]$^+$: *m*/*z* 1044.4183 (calcd for [$C_{48}H_{66}{}^{172}YbN_5O_{10}$]$^{2+}$, 1044.4174). Anal. Calcd for [$C_{48}H_{66}YbN_5O_{10}$]$(OAc)_2(H_2O)$: C, 52.83; H, 6.31; N, 5.92; Yb, 14.64. Found: C, 52.74; H, 6.07; N, 5.89; Yb, 15.00.

Lutetium(III) Complex 7. The synthesis of this complex has been previously described in detail; see ref 42.

Yttrium(III) Complex 8. The hydrochloride salt of macrocycle **11** (4.4 g, 4.8 mmol), $Y(OAc)_3 \cdot 4H_2O$ (1.95 g, 6.0 mmol), and triethylamine (4.9 g, 48.4 mmol) were mixed together in methanol (300 mL), and the mixture was heated to reflux in the air. Using the general procedure described above, the reaction was deemed complete after 5.5 h. After workup and recrystallization from ethanol/*n*-heptane as described above, 3.8 g (73%) of **8** was obtained in the form of a dark green microcrystalline solid. UV/vis [(λ_{max}, nm for Soret-type absorption band, in 96% MeOH/4% acetic acid) (log ϵ)]: 475 nm (5.10) FAB MS, [M − 2OAc$^-$]$^+$: *m*/*z* 962. HRMS, [M − 2OAc$^-$]$^+$: *m*/*z* 961.3840 (calcd for [$C_{48}H_{66}YN_5O_{10}$]$^{2+}$, 961.3868). Anal. Calcd for [$C_{48}H_{66}YN_5O_{10}$]$(OAc)_2(H_2O)_{1/2}$: C, 57.35; H, 6.76; N, 6.43; Y, 8.16. Found: C, 57.41; H, 6.35; N, 6.52; Y, 8.11.

Cadmium(II) Complex 9. The hydrochloride salt of macrocycle **11** (2.0 g, 2.2 mmol), $Cd(OAc)_2 \cdot 2H_2O$ (0.70 g, 2.6 mmol), and triethylamine (2.2 g, 22 mmol) were mixed together in methanol (400 mL), and the mixture was heated to reflux in the air. Using the general procedure described above, the reaction was deemed complete after 16 h. The solvent was removed under reduced pressure, and the solids were dried in vacuo. The crude complex was chromatographed on normal phase silica gel using as the eluent first neat chloroform and then increasing concentrations of methanol in chloroform up to neat methanol. The green complex was collected, solvent removed under reduced pressure, and the solid dried in vacuo to yield 1.0 g (44%) of **9** as a dark green microcrystalline solid. UV/vis [(λ_{max}, nm for Soret-type and Q-type absorption bands, in 96% MeOH/4% acetic acid) (log ϵ)]: 464 nm (5.07) and 733 (4.61); FAB MS, [M − OAc$^-$]$^+$: *m*/*z* 986; HRMS, [M − OAc$^-$]$^+$: *m*/*z* 982.3844 (calcd for [$C_{48}H_{66}{}^{110}CdN_5O_{10}$]$^+$, 982.3840). Anal. Calcd for [$C_{48}H_{66}CdN_5O_{10}$](OAc): C, 57.49; H, 6.66; N, 6.70; Cd, 10.76. Found: C, 57.26; H, 6.79; N, 6.65; Cd, 10.48.

Indium(III) Complex 10. The hydrochloride salt of macrocycle **11** (1.5 g, 1.64 mmol), $In(OAc)_3 \cdot xH_2O$ (0.72 g, 1.97 mmol), and triethylamine (1.7 g, 16.4 mmol) were mixed together in methanol (300 mL), and the mixture was heated to reflux in the air. Using the general procedure described above, the reaction was deemed complete after 6 h. After workup and recrystallization from ethanol/*n*-heptane as described above, 0.9 g (50%) of **10** was obtained in the form of a dark green microcrystalline solid. UV/vis [(λ_{max}, nm for Soret-type and Q-type absorption bands, in 96% MeOH/4% acetic acid) (log ϵ)]: 470 nm (5.10), 730 nm (4.54). FAB MS, [M − 2OAc$^-$]$^+$: *m*/*z* 987. HRMS, [M − 2OAc$^-$]$^+$: *m*/*z* 987.3843 (calcd for [$C_{48}H_{66}{}^{115}InN_5O_{10}$]$^{2+}$, 987.3848). Anal. Calcd for [$C_{48}H_{66}$-InN_5O_{10}]$(OAc)_2(H_2O)$: C, 55.57; H, 6.64; N, 6.23; In, 10.22. Found: C, 55.67; H, 6.60; N, 6.31; In, 10.54.

Results and Discussion

Cyclic Voltammetry. The lanthanide(oid) texaphyrin complexes (**2**, **3**, **4**, **7**, and **9**) all display two quasi-reversible one-electron reductions at similar first ($E_{1/2}{}^a$ −270 mV vs Ag/AgCl) and second ($E_{1/2}{}^a$ −750 mV vs Ag/AgCl) potentials in deoxygenated DMF (Table 1). The unfavorably high reduction potentials for the lanthanide M(III)/M(II) couples[52] lead to the assumption that the reduction occurs on the texaphyrin ligand,

TABLE 1: Electrochemical Potentials (vs Ag/AgCl) for the Cyclic Voltammetric Reduction of M−Tex$^{+/2+}$ Complexes in DMF (0.1 M Tetrabutylammonium Perchlorate, 200 mV/s)

compound	reduction I $E_{1/2}$ (mV)	reduction II $E_{1/2}$ (mV)
Gd−Tex^{2+}	−263	−757
Eu−Tex^{2+}	−267	−753
Dy−Tex^{2+}	−269	−748
Lu−Tex^{2+}	−266	−725
Y−Tex^{2+}	−286	−746
Cd−Tex^{+}	−576	−982

rather than at the metal center. The metal independence of the reduction potentials is considered consistent with this conclusion. In this context, it should be noted that the reduction potential of the Cd(II) texaphyrin (**9**) is cathodically shifted relative to the lanthanide complexes. This shift in potential is believed to reflect differences in the electrostatics of the metal−ligand rather than a reduction process occurring at the metal center (see Pulse Radiolysis section below).

Attempts to obtain a reproducible, across-the-lanthanide series of reduction potentials in H_2O from cyclic voltammetric studies proved unsuccessful under a variety of conditions. This lack of success can be rationalized, at least in part, in terms of the high instability of the redox products evolving from the one-electron reduction processes.[53] In particular, protonation of the singly reduced texaphyrins could serve to shorten the lifetimes of the one-electron reduced texaphyrins (see Pulse Radiolysis section below). In light of such concerns, electrochemical measurements were made in a solvent that largely precludes protonation, namely isopropyl alcohol. Cyclic voltammograms obtained under these conditions proved to be similar to those recorded in DMF. However, the addition of water to the isopropyl alcohol solutions acted to diminish the reversibility of the two redox steps mentioned above.

Pulse Radiolysis. Pulse radiolytic analyses are often used to model radiation therapy since it generates the same radical species as are believed to be produced in cells undergoing XRT.[11] Furthermore, the time resolution and the possibility of selectively forming either hydrated electrons ("reducing" conditions) or hydroxyl radicals ("oxidizing" conditions) allows for measurement of the reaction kinetics under conditions where these two reactive intermediates exist to near exclusion.[54] Under the current experimental conditions the reactive radical species $^{\bullet}H$, $^{\bullet}OH$, $e^-(aq)$ are produced in addition to the following molecular products: H_2, H_2O_2, and $H^+(aq)$ (see eq 1).

$$H_2O \xrightarrow{\text{X-ray}} {}^{\bullet}OH + e^-(aq) + H_3O^+ + {}^{\bullet}H + H_2 + H_2O_2 \quad (1)$$

Addition of *tert*-butyl alcohol to a deoxygenated aqueous solution leads to a quantitative conversion of $^{\bullet}OH$ radicals into the redox-inert 2,2-dimethyl-2-hydroxyethyl radical (eq 2). This leaves a higher relative concentration of $e^-(aq)$ that, inter alia, can reduce the metallotexaphyrin (eq 3). On the other hand,

$$(CH_3)_3COH + {}^{\bullet}OH \rightarrow {}^{\bullet}CH_2(CH_3)_2COH + H_2O \quad (2)$$

$$M-Tex^{2+} + e^-(aq) \rightarrow M-Tex^{\bullet+} \quad (3)$$

saturation with N_2O serves to scavenge the solvated electrons, yielding a second crop of hydroxyl radicals (eq 4). These latter species are then available to react with the texaphyrin to form, presumably, an oxidized texaphyrin species (eq 5).

$$N_2O + e^-(aq) + H_2O \rightarrow N_2 + {}^{\bullet}OH + {}^{-}OH \quad (4)$$

$$M-Tex^{2+} + {}^{\bullet}OH \rightarrow M-Tex^{\bullet 3+} + {}^{-}OH \quad (5)$$

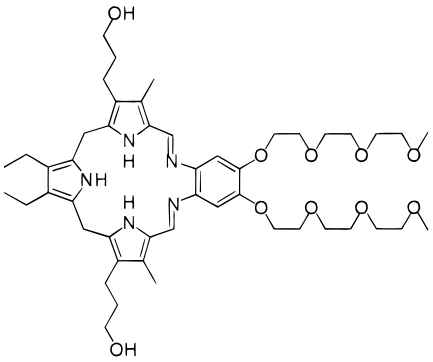

11

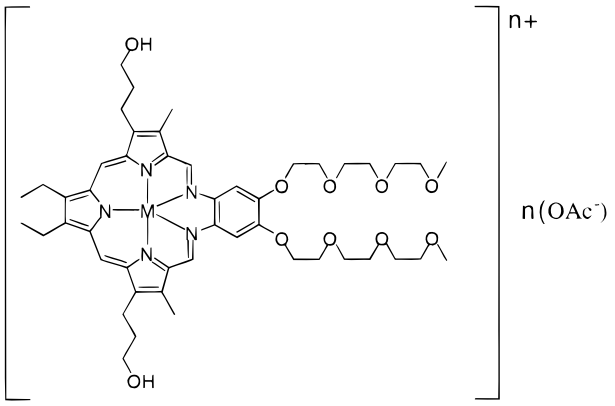

1 M = H; n = 0
2 M = Gd; n = 2
3 M = Eu; n = 2
4 M = Dy; n = 2
5 M = Tm; n = 2
6 M = Yb; n = 2
7 M = Lu; n = 2
8 M = Y; n = 2
9 M = Cd; n = 1
10 M = In; n = 2

Figure 1. Structures of the complexes discussed in this report and the metal-free reduced macrocyclic precursor from which they were derived.

Reduction Chemistry. Under anaerobic reducing conditions (eqs 2 and 3) all of the metallotexaphyrins tested [M = Y(III) **8**, Cd(II) **9**, In(III) **10**, Gd(III) **2**, Eu(III) **3**, Dy(III) **4**, Tm(III) **5**, Yb(III) **6**, and Lu(III) **7**] yielded similar differential absorption spectra with intense ground-state bleaching in the region corresponding to the Q-like band (ca. 730 nm) and broad absorptions centered around 830 nm (see Table 2). Figure 2a displays, for example, the differential absorption spectrum observed upon reduction of Gd−Tex^{2+} in N_2-saturated aqueous Na_2HPO_4 buffer solution.

It is well documented that ligand-centered reduction of porphyrins,[55,56] porphycenes,[57,58] and corrphycenes[59] gives rise to a broad absorption in the 700−840 nm range. In contrast, metal-centered reductions of these macrocyclic complexes lead only to minor shifts in the associated Soret- and Q-bands.[57,59,60] Therefore, on the basis of this precedent the broad absorption observed upon radiolysis of the metallotexaphyrins is ascribed to a reduction process occurring on the texaphyrin ligand, and not at the metal center. For the trivalent metal cation complexes, this yields the π-radical cation, M−Tex$^{\bullet+}$. This presumed ligand-based reduction is supported by the metal independence of the reduction potentials and the unfavorability of the M(III)/M(II) reduction process mentioned above.

The reaction dynamics of M−Tex^{2+} with $e^-(aq)$ were

TABLE 2: Rate Constants for the Reduction, Protonation, Dimerization, and Oxidation of Various M−Tex$^{+/2+}$ and Absorption Maxima for the Resulting Redox Products (M−Tex$^{\bullet+}$, Cd−Tex$^{\bullet}$ and M−Tex$^{\bullet 3+}$, Cd−Tex$^{\bullet 2+}$)[a]

compound	$M^{2+/3+}$ radius (Å)[63]	$k_{(e^-(aq))}$[d] (10^9 M^{-1} s^{-1})	λ_{max} M−Tex$^{\bullet+}$ (nm)	$k_{(^{\bullet}OH)}$[e] (10^9 M^{-1} s^{-1})	λ_{max} M−Tex$^{\bullet 3+}$ (nm)	$k_{(H^+)}$[f] (10^8 M^{-1} s^{-1})	$k_{dimerization}$[g] (10^7 M^{-1} s^{-1})
Y−Tex^{2+} [b]	0.985	64	830	3.5	820	9.1	2.7
Eu−Tex^{2+} [c]	1.066	41	830	7.4	820	12	13
Gd−Tex^{2+} [c]	1.053	63	820	4.8	810	10	5.9
Dy−Tex^{2+} [c]	1.027	47	830	5.7	820	8.5	4.0
Tm−Tex^{2+} [c]	0.994	68	820	3.8	830		4.7
Yb−Tex^{2+} [c]	0.985	37	820	6.7	830	0.8	2.9
Lu−Tex^{2+} [b]	0.977	40	830	5.1	840	1.5	2.7
In−Tex^{2+} [b]	0.92	56	840	2.5	830		0.4
Cd−Tex^{+} [b]	1.10	44	830	6.3	850		0.3

[a] ±10% overall error. [b] Diamagnetic. [c] Paramagnetic. [d] Rate constant for reaction with $e^-_{(aq)}$. [e] Rate constant for reaction with $^{\bullet}OH$. [f] Rate constant of protonation of the one-electron reduced metallotexaphyrins. [g] Rate-constant for dimerization of the protonated species.

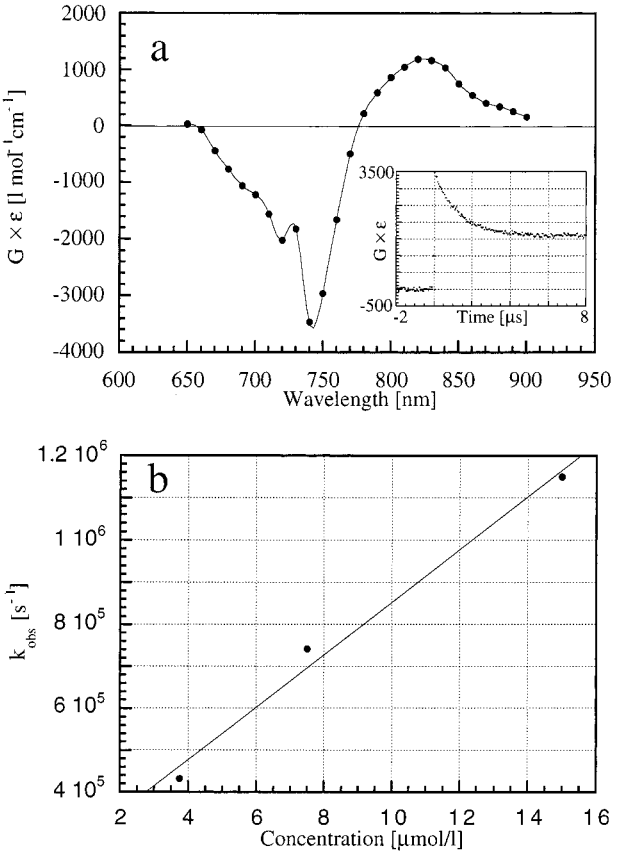

Figure 2. (a) Transient absorption spectrum of Gd−Tex$^{\bullet+}$ obtained upon pulse radiolytic treatment of a 1.0×10^{-5} M solution of Gd−Tex^{2+} in nitrogen-saturated aqueous Na_2HPO_4 buffer (pH 8.7) (2 vol % *tert*-butyl alcohol). Inset: Time−absorption profile for the grow-in of the transient (λ_{max} at 830 nm) ascribed to Gd−Tex$^{\bullet+}$. (b) Plot of k_{obs} vs [Gd−Tex^{2+}] at 720 nm (e^-(aq)) for the reduction of Gd−Tex^{2+}, in deoxygenated aqueous solution (2 vol % *tert*-butyl alcohol) (intercept = 2.3×10^5; slope = 6.3×10^{10}; $r^2 = 0.99$).

followed by monitoring the decay of the hydrated electron absorption band around 720 nm and the growth of the reduced texaphyrin absorption at 830 nm. The observed rates were linearly dependent upon the M−Tex^{2+} concentration in the range between 3.7 and 15 μM (see Figure 2b). Linear least squares iterations provided the pseudo-first-order rate constants. The rate constants for electron capture by all of the M−Tex^{2+} complexes (in 2.0 mM aqueous Na_2HPO_4, pH 8.7) were, as illustrated in Table 2, very similar and were found to range from 40×10^9 M^{-1} s^{-1} to 63×10^9 M^{-1} s^{-1}. It should be noted that similar kinetic parameters were obtained whether it was the bleaching or grow-in processes that were monitored over the course of the observed spectral region (500−900 nm).

Experiments carried out in 2-propanol, ethanol, and methanol yielded similar spectral features. This leads to the conclusion that metallotexaphyrins are also reduced by $(CH_3)_2{}^{\bullet}COH$, $CH_3{}^{\bullet}CHOH$, and $^{\bullet}CH_2OH$, even though the rates of reduction with these radicals are slightly slower than with e^-(aq) ($k = 5.2 \times 10^9$ M^{-1} s^{-1} and $k = 3.8 \times 10^9$ M^{-1} s^{-1} for 2-propanol and methanol, respectively; errors ±10%).

The singly reduced texaphyrin decays rapidly into one or more species that are different from the original texaphyrin. To determine the decay pathway of the singly reduced texaphyrin, measurements were made at various pH values and in D_2O. Also, dose dependence experiments were carried out.

In aqueous Na_2HPO_4 buffered solution (pH 8.7), the singly reduced texaphyrin exhibited a rapid decay with a lifetime of, for example, 18.8 μs in the case of Gd−Tex^{2+}. The differential absorption spectrum of the resulting species, as depicted in Figure 3, is, however, very similar to its precursor, namely the one-electron reduced product. Variation of the proton concentration, e.g., decreasing the pH, resulted in an increase in the rate of decay of the singly reduced texaphyrin. On the basis of this dependence, and in accord with earlier results,[43] this process is ascribed to protonation of the initially formed singly reduced texaphyrin. Consistent with this assignment is the finding that the proposed protonation is approximately a factor of 4 slower in D_2O (with a half-life of 79.4 μs for Gd−Tex$^{\bullet+}$) relative to H_2O solutions (Figure 3b); this points to a relatively large isotope effect. The protonation rates, collated in Table 2, vary for the different metal ion complexes and range from 1.0×10^9 M^{-1} s^{-1} (±10%) for Gd−Tex^{2+} to 1.5×10^8 M^{-1} s^{-1} (±10%) for Lu−Tex^{2+}. The isotope effects also vary, being for instance 2, rather than 4, in the case of Lu−Tex^{2+}.

Protonation in neutral solutions is overshadowed, in part, by the onset of another decay process that commences before the initial protonation is complete. Prior work with metalloporphyrins[55,56] led us to consider, as working hypotheses, that these decay processes could involve reactions of the reduced protonated species with unreduced M−Tex^{2+} (e.g., "dimer" formation) and/or disproportionation, as illustrated in eqs 6 and 7, respectively.

$$\text{M}-\text{TexH}^{\bullet 2+} \xrightarrow{\text{M}-\text{Tex}^{2+}} (\text{M}-\text{Tex})_2\text{H}^{\bullet 4+} \quad (6)$$

$$\text{M}-\text{TexH}^{\bullet 2+} \xrightarrow{\text{M}-\text{TexH}^{\bullet 2+}} \text{M}-\text{TexH}^{+} + \text{M}-\text{Tex}^{2+} + \text{H}^{+} \quad (7)$$

The lifetimes of all the M−TexH$^{\bullet 2+}$complexes suffered remarkable reductions with increasing concentration. In our present study the M−Tex^{2+} concentration was varied over a wide range [$(2-100) \times 10^{-6}$ M], and the decay in question was, in fact, found to involve a pseudo-first-order process at high concentrations. This leads us to propose that M−TexH$^{\bullet 2+}$

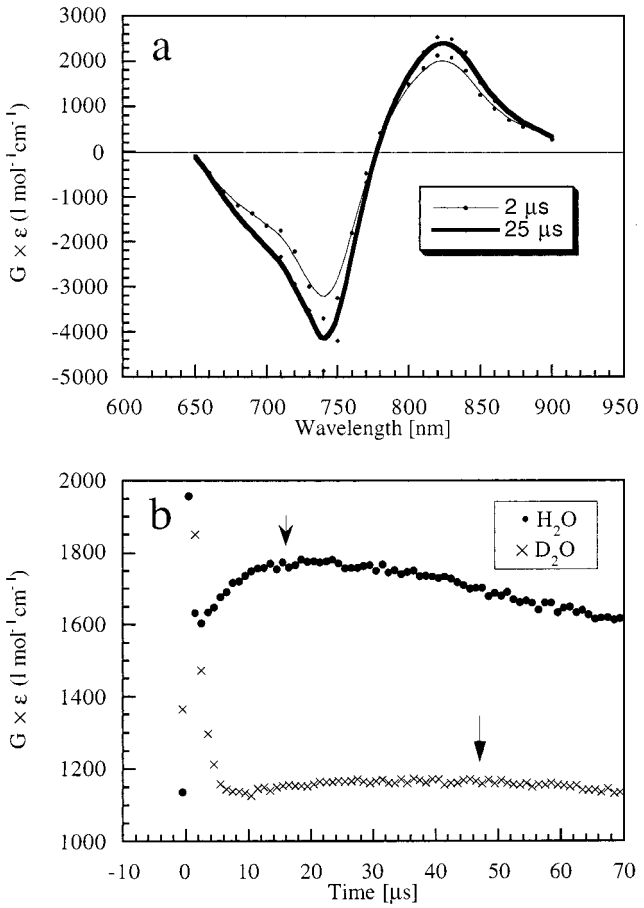

Figure 3. (a) One-electron reduction. Transient absorption spectrum of Gd−Tex$^{\bullet+}$ (2.5 μs after the pulse) and its protonated form Gd−TexH$^{\bullet 2+}$ (5 μs after the pulse) recorded in nitrogen-saturated aqueous Na_2HPO_4 buffer solution (pH 8.7) (2 vol % *tert*-butyl alcohol). (b) Isotope effect: time-absorption profile for the protonation process of Gd−Tex$^{\bullet+}$ (1.0×10^{-5} M) in H_2O and D_2O solutions, respectively. The arrows highlight the end points of protonation.

reacts with ground-state M−Tex^{2+}, at least under these latter conditions; the bimolecular rate constants for this reaction, as derived from $k = \ln 2/t_{1/2}$ vs [M−Tex^{2+}] plots, range from 5.9×10^7 M^{-1} s^{-1} for Gd−TexH$^{\bullet 2+}$ to 2.7×10^7 M^{-1} s^{-1} for Lu−TexH$^{\bullet 2+}$.

At lower M−Tex^{2+} concentrations ($<1 \times 10^{-5}$ M) the decay kinetics became second order for most of the complexes. Further evidence for this proposed second-order behavior and thus, in turn, for a possible disproportionation reaction came from radiation dose dependence studies. The lifetime of the protonated singly reduced species at high Gd−Tex^{2+} concentration is, for instance, insignificantly impacted by a change in the radiation dose (1×10^{-4} M Gd−Tex^{2+}: $t = 176$ μs at 4.0×10^{-6} M radicals; $t = 169$ μs at 8.0×10^{-6} M radicals). Only at low Gd−Tex^{2+} concentrations is the decay effectively influenced by changes in the radiation dose. For example, at a given concentration of 1.0×10^{-5} M Gd−Tex^{2+}, a lifetime of 860 μs was observed at a radical concentration of 4.0×10^{-6} M. By contrast, at this same concentration of Gd−Tex^{2+}, a t value of 332 μs was recorded at a radical concentration of 8.0×10^{-6} M.

To the extent that disproportionation constitutes the sole pathway for Gd−TexH$^{\bullet 2+}$ decay, a 4-fold change in lifetime is expected upon a 2-fold lowering of the radiation dose. This leads to the conclusion that the overall deactivation process is governed by two competing reactions, namely (1) disproportionation and (2) reaction of Gd−TexH$^{\bullet 2+}$ with another ground-state Gd−Tex^{2+} species (eqs 7 and 6, respectively), with the latter pathway generally dominating.

In contrast to what is true for the Gd−Tex^{2+} complex, the decay of the intermediate Lu−TexH$^{\bullet 2+}$ species does not appear to vary appreciably with radiation dose. This lack of radiation dose dependence for Lu−Tex^{2+} might reflect a preferential decay via dimer formation (i.e., reaction with another unreduced Lu−Tex^{2+}) rather than a decay process occuring through a combination of disproportionation and dimerization. Some support for this suggested decay pathway comes from the observation that Lu−Tex^{2+} will aggregate, even in the ground state.[42]

Further substantiation for the proposal that various protonated one-electron reduced M−TexH$^{\bullet 2+}$ species, including the respective Gd−Tex^{2+} and Lu−Tex^{2+} complexes, react with ground-state M−Tex^{2+} emerges from reduction experiments carried out in micellar solutions. Introducing surfactants should ensure that the original ground-state texaphyrin is monomeric. Such monomerization, in turn, should decrease the assumed dimerization rate. As it transpired, the lifetimes of Gd−TexH$^{\bullet 2+}$ and Lu−TexH$^{\bullet 2+}$ were found to increase in the respective surfactant solutions. Interestingly, the use of micellar media also serves to slow the initial protonation process, yielding half-lives on the order of 75 μs for Gd−Tex$^{\bullet+}$, rather than the 18.8 μs observed in homogeneous solution.

Once formed, the presumed dimer is considered susceptible to yet another decay process for which the relevant rate constants are typically on the order of $(4.8-9.8) \times 10^5$ M^{-1} s^{-1}. Currently, the exact nature of this follow-up decay remains recondite. It is tentatively ascribed to a protonation process, based on the fact that an increase in the decay rate is observed at lower pH.

Oxidation Chemistry. Pulse radiolysis of M−Tex^{2+} under strictly oxidizing conditions (see eqs 4 and 5) leads to a grow-in of broad absorption features in the 780−900 nm spectral region, as illustrated for Gd−Tex^{2+} in Figure 4a (see also Table 2). This spectral behavior bears analogy to what is seen in the case of several porphyrin[55,56] and porphycene[57,58] analogues. In these latter instances, ligand oxidation gives rise to broad absorption features between 700 and 840 nm.

On the basis of the above analogy, it is hypothesized that, upon reaction with $^{\bullet}$OH ($E_{1/2} = 2.7$ V vs NHE (2.48 V vs Ag/AgCl) under acidic conditions and $E_{1/2} = 1.8$ V vs NHE (1.58 V vs Ag/AgCl) in neutral solution),[61] the texaphyrin ligand is oxidized, forming the π-radical cation M−Tex$^{\bullet 3+}$. To confirm that the observed spectral changes are indeed appropriately ascribed to an oxidation event, rather than to, e.g., direct addition of $^{\bullet}$OH to the macrocyclic texaphyrin periphery, an experiment was performed under $^{\bullet}$OH-free oxidizing conditions. Specifically, Cl^- was added to the reaction media (pH = 3.2) so as to convert any $^{\bullet}$OH to the strongly oxidizing species, $Cl_2^{\bullet-}$ ($E_{1/2} = 2.2$ V vs NHE)[61] (see eq 8). This species is considered much less likely to add to the texaphyrin periphery.[60,62]

$$^{\bullet}OH + Cl^- \rightarrow {}^-OH + Cl^{\bullet} \xrightarrow{Cl^-} Cl_2^{\bullet-} \qquad (8)$$

In terms of experiment, the differential absorption spectrum recorded with, for example, Gd−Tex^{2+} under $Cl_2^{\bullet-}$ oxidative conditions was in excellent agreement with that obtained when $^{\bullet}$OH was used as the sole reactive species. In fact, $Cl_2^{\bullet-}$ and $^{\bullet}$OH were both found to give rise to absorption maxima at 830 nm with intensities of $G \times \epsilon$ of 960 and 1000, respectively. This supports the above assumption that $^{\bullet}$OH radical acts only as an electron-transfer oxidant in its reactions with this particular metallotexaphyrin.

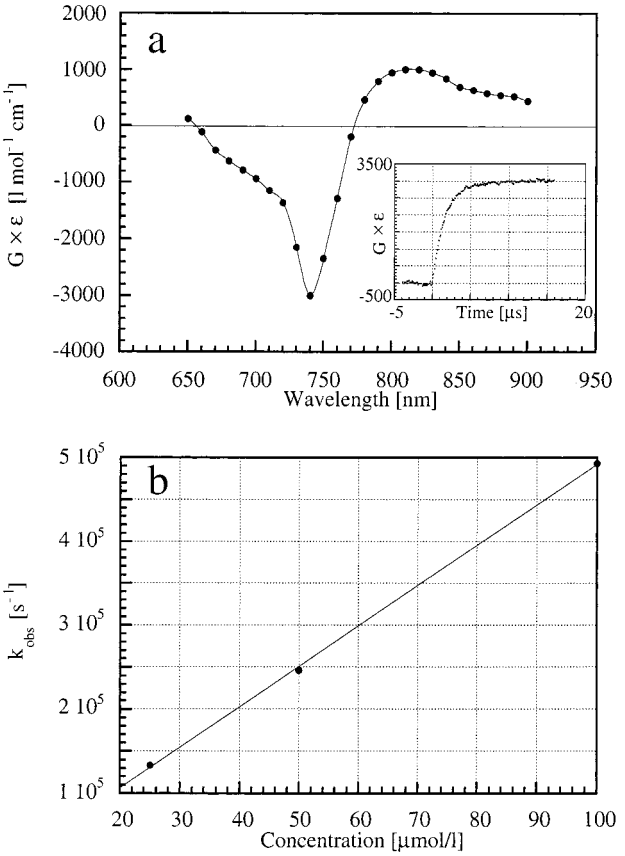

Figure 4. (a) One-electron oxidation. Transient absorption spectrum of Gd−Tex$^{\bullet 3+}$ obtained upon pulse radiolytic treatment of a 1.0×10^{-5} M solution of Gd−Tex^{2+} in N_2O-saturated aqueous Na_2HPO_4 buffer (pH 8.7). Inset: time−absorption profile for the grow-in of the transient (λ_{max} at 810 nm) ascribed to Gd−Tex$^{\bullet 3+}$. (b) Plot of k_{obs} vs [Gd−Tex^{2+}] at 830 nm for the oxidation of Gd−Tex^{2+} by $^{\bullet}$OH, in N_2O-saturated aqueous solution (intercept = 9.5×10^3; slope = 4.8×10^9; $r^2 = 0.99$).

Relevant to the above conclusion is the finding that adding the carbon centered radical $^{\bullet}CH_2(CH_3)_2COH$ to Gd−Tex^{2+}, in the absence of $Cl_2^{\bullet -}$ and $^{\bullet}$OH, failed to produce the characteristic spectral features described above. In particular, no maximum around 830 nm was observed under these particular experimental conditions (N_2O saturated aqueous solutions containing 2 vol % *tert*-butyl alcohol). This negative control lends credence to the idea that $^{\bullet}$OH and $Cl_2^{\bullet -}$ act as pure oxidants.

The pseudo-first-order rate constants for reaction of M−Tex^{2+} with $^{\bullet}$OH were determined in a manner similar to that used to obtain the rate constants for reaction of M−Tex^{2+} with e^-(aq), i.e., from the grow-in kinetics of the 830 nm absorption feature (Figure 4b). Interestingly, as illustrated in Table 2, all of the metallotexaphyrins display similar rate constants for reaction with $^{\bullet}$OH (the relevant values range from 2.5×10^9 M^{-1} s^{-1} to 7.3×10^9 M^{-1} s^{-1}; estimated errors ±10%).

Origin of Reductive Differences. The difference in the stability of the singly reduced metallotexaphyrins could be due to several factors. Two of the more obvious with which we were primarily concerned involve the spin of the metals (paramagnetic vs diamagnetic) and the size of metal cation (ranging from 0.977 Å for Lu(III) to 1.10 Å for Cd(II)).[63] The magnetism of the central metal could influence the reactivity of the singly reduced texaphyrin. Likewise, it is also feasible that the metal size governs the stability and, in turn, the reactivity of the singly reduced species. Prior X-ray crystallographic analysis of Gd−Tex^{2+}, Eu−Tex^{2+}, and Lu−Tex^{2+} complexes show that, for nitrate and methanol donor ligands, the larger Gd(III) and Eu(III) cations are situated approximately 0.6 Å above the macrocyclic N_5 plane.[35,38] By contrast, for the same ancillary ligand set, the smaller Lu(III) cation is found to be located out of the plane by only ca. 0.27 Å.[35,38] The texaphyrin ligand itself is also found to be less distorted from planarity in the case of the lutetium(III) complex than in the case of the europium(III) and gadolinium(III) complexes.

For the diamagnetic complexes, it can, for example, be seen that the protonation rate is rather slow for Lu−Tex^{2+}, but fast for Y−Tex^{2+}. For the paramagnetic species, the protonation is generally very fast. To the extent that the data set of paramagnetic and diamagnetic complexes is large enough to allow conclusions to be drawn, it is easy to see that no clear correlation exists between the spin state of the coordinated metal cation and the susceptibility of the singly reduced texaphyrins toward protonation.

Since the observed trend hinders a meaningful correlation with the spin state, a comparison with the metal size was undertaken. Table 2, although comprising a limited data set, shows that the reduced forms of the complexes that contain large trivalent lanthanides (i.e., Gd(III) and Eu(III)) protonate rapidly, whereas the reduced forms of those complexes containing small trivalent lanthanides (i.e., Lu(III) and Yb(III)) are protonated almost one order of magnitude slower than the congeneric complexes containing a larger cation.[64] Out of plane displacement of the larger metal ions cause the texaphyrin core to pucker to a larger extent than is true for the smaller analogues.[38] This distortion, which would necessarily be reflected in a weakened π-delocalization and greater susceptibility toward reaction with an electrophile, is expected to facilitate protonation of the M−Tex$^{\bullet +}$ species.

The above results, and in particular the one order of magnitude difference in protonation rate, may help explain the difference in radiation sensitizing observed when Gd−Tex^{2+} and Lu−Tex^{2+} are studied under identical biological conditions. Indeed, the present results lead us to suggest that one explanation for why Gd−Tex^{2+} is more efficacious than Lu−Tex^{2+} is that the singly reduced form of the gadolinium complex is protonated too rapidly to allow for further follow-up reaction with hydroxyl radicals. By contrast, the singly reduced product produced from the starting lutetium complex may be long-lived enough to react with the hydroxyl radicals. This latter species, but not Gd−Tex^{2+}, would thus act to decrease the effective concentration of $^{\bullet}$OH. Since $^{\bullet}$OH is implicated as being a major cytotoxin responsible for the therapeutic effect of radiation therapy, the fact that less would be available in the case of Lu−Tex^{2+} could account for why it is a less effective sensitizer than Gd−Tex^{2+} in vivo. Studies designed to confirm or refute the chemical viability of this proposed explanation are currently underway.

Acknowledgment. This work was supported in part by the Office of Basic Energy Sciences of the U.S. Department of Energy (grant No. NDRL-4047 from the Notre Dame Radiation Laboratory) and the National Institutes of Health (CA 68682 to J.L.S.). W.E.A. thanks the American Cancer Society for a Postdoctoral Fellowship. We are grateful to Alice Lin, Cristina Montes, and Li Ma for their help with HPLC analyses and extinction coefficient measurements of the metallotexaphyrin complexes. We wish to thank Drs. Maria Dulay, Richard Miller, Darren Madga, Kathryn Woodburn, Dales Miles, and Ms. Diann Nagami for their review of this manuscript. We also wish to thank Jason Rao for his synthetic assistance on this project.

References and Notes

(1) Cancer Facts and Figures-1997. American Cancer Society: Atlanta, GA, 1997.

(2) Otto, S. E. *Pocket Guide to Oncology Nursing*; Mosby-Year Book, Inc.: St. Louis, 1995.
(3) Gates, R. A.; Fink, R. M. *Oncology Nursing Secrets*; Hanley & Belfus, Inc.: Philadelphia, 1997.
(4) Hall, E. J. *The Oxygen Effect and Reoxygenation*; J. B. Lippincott Co.: Philadelphia, 1994; pp 133−152.
(5) Thomlinson, R. H.; Gray, L. H. *Br. J. Cancer* **1955**, *9*, 539−549.
(6) Coutard, H. *Lancet* **1934**, *2*, 1−12.
(7) Felmeier, J. J. In *Radiation Oncology*; Weiss, G. R., Ed.; Appleton & Lange: Norwalk, CT, 1993; pp 74−88.
(8) Watson, E. R.; Halnan, K. E.; Dische, S.; Saunders, M. I.; Cade, I. S.; McEwan, J. B.; Wienik, F.; Perrins, D. J. D.; Sutherland, I. *Br. J. Radiol.* **1978**, *51*, 879−887.
(9) Shenoy, M. A.; Singh, B. B. *Cancer Invest.* **1992**, *10*, 533−551.
(10) Hendrickson, F. R.; Withers, H. R. In *Principles of Radiation Oncology*; Holleb, A. I., Fink, D. J., Murphy, G. P., Eds.; American Cancer Society: Washington, DC, 1991; pp 35−37.
(11) Russo, A.; Mitchell, J.; Kinsella, T.; Morstyn, G.; Glatsetin, E. *Semin. Oncol.* **1985**, *12*, 332−349.
(12) Goffman, T. E.; Dachowski, L. J.; Bobo, H.; Oldfield, E. H.; Steinberg, S. M.; Cook, J.; Mitchell, J. B.; Katz, D.; Smith, R.; Glatstein, E. *J. Clin. Oncol.* **1992**, *10*, 264−268.
(13) Robertson, J. M.; Ensminger, W. D.; Walker, S.; Lawrence, T. S. *Int. J. Radiat. Oncol. Biol. Phys.* **1997**, *37*, 331−335.
(14) Dische, S. *Radiother. Oncol.* **1985**, *3*, 97−115.
(15) Dische, S. *Int. J. Radiat. Oncol. Biol. Phys.* **1989**, *16*, 1057−1060.
(16) Abratt, R. O.; Craighead, P.; Reddi, V. B.; Sarembock, L. A. *Br. J. Cancer* **1991**, *64*, 968−970.
(17) Baillet, F.; Housset, M.; Dessard-Diana, B.; Boisserie, G. *Int. J. Radiat. Oncol. Biol. Phys.* **1989**, *16*, 1073−1075.
(18) Brown, J. M. *Int. J. Radiat. Oncol. Biol. Phys.* **1989**, *16*, 98−993.
(19) Chassagne, D.; Sancho-Garnier, H.; Charreau, I.; Eschwege, F.; Malaise, E. P. *Radiother. Oncol. Suppl.* **1991**, *20*, 121−127.
(20) Chassagne, D.; Charreau, I.; Sanco-Garnier, H.; Eschwege, F.; Malaise, E. P. *Int. J. Radiat. Oncol. Biol. Phys.* **1992**, *22*, 581−584.
(21) Coleman, C. N.; Urtasan, R. C.; Wasserman, T. H.; Hancok, S.; Harris, J. W.; Kirst, V. K. *Int. J. Radiat. Oncol. Biol. Phys.* **1984**, *10*, 1749−1753.
(22) Coleman, C. N.; Wasserman, T. H.; Urtasun, R. C.; Halsey, J.; Hirst, V. K.; Hancock, S.; Phillips, T. L. *Int. J. Radiat. Oncol. Biol. Phys.* **1986**, *12*, 1105−1108.
(23) Coleman, C. N.; Halsey, J.; Cox, R. S.; Hirst, V. C.; Blasahke, T.; Howes, A. E.; Wasserman, T. H.; Urtasun, R. C.; Pajak, T.; Hancock, S.; Phillips, T. L.; Noll, L. *Cancer Res.* **1987**, *47*, 319−322.
(24) Dische, S.; Saunders, M. I.; Bennett, M. H.; Chir, B.; Dunphy, E. P.; Des Rochers, C.; Straford, M. R. L.; Minchinton, A. I.; Wardman, P. A. *Br. J. Radiol.* **1986**, *59*, 911−917.
(25) Fazekas, J.; Pajak, T. F.; Wasserman, T.; Marcial, V.; Davis, L.; Kramer, S.; Rotman, M.; Stetz, J. *Int. J. Radiat. Oncol. Biol. Phys.* **1987**, *13*, 1155−1160.
(26) Komarnicky, L. T.; Phillips, T. L.; Martz, K.; Asbell, S.; Isaacson, S.; Urtasun, R. *Int. J. Radiat. Oncol. Biol. Phys.* **1991**, *20*, 53−58.
(27) Newman, H. F. V.; Ward, R.; Workman, P.; Bleehen, N. M. *Int. J. Radiat. Oncol. Biol. Phys.* **1988**, *15*, 1073−1083.
(28) Saunders, M. I.; Anderson, P. J.; Bennett, M. H.; Dische, S.; Minchinton, A.; Stratford, M. R.; Tothill, M. *Int. J. Radiat. Oncol. Biol. Phys.* **1984**, *10*, 1759−1763.
(29) Shulman, L. N.; Buswell, L.; Kalish, L.; Coleman, C. N. *Int. J. Radiat. Oncol. Biol. Phys.* **1994**, *29*, 541−543.
(30) Shulman, L. N.; Buswell, L.; Goddman, H.; Muto, M.; Berkowitz, R.; Teicher, B.; Kusumoto, T.; Hurwitz, S. J.; Kalish, L. A.; Coleman, C. N. *Int. J. Radiat. Oncol. Biol. Phys.* **1994**, *29*, 545−548.
(31) Kaplan, H. S. *Proc. Natl. Acad. Sci. U.S.A.* **1966**, *55*, 1442−1446.
(32) Dewey, W. C.; Humphrey, R. M. *Radiat. Res.* **1965**, *26*, 538−553.
(33) Hall, E. J. *Cell Survival Curves*; J. B. Lippincott Co.: Philadelphia, 1994; pp 29−43.
(34) Brown, J. M. In *Electron Affinic Agents: Development of the Optimum Radiosensitizer and Chemosensitizer for Clinical Applications*; Sugahara, T., Ed.; Academic: San Francisco, 1984; pp 139−176.
(35) Sessler, J. L.; Hemmi, G.; Mody, T. D.; Murai, T.; Burrell, A.; Young, S. W. *Acc. Chem. Res.* **1994**, *27*, 43−50.
(36) Sessler, J. L.; Murai, T.; Lynch, V.; Cyr, M. *J. Am. Chem. Soc.* **1988**, *110*, 5586−5588.
(37) Sessler, J. L.; Murai, T.; Hemmi, G. *Inorg. Chem.* **1989**, *28*, 3390−3393.
(38) Sessler, J. L.; Mody, T. D.; Hemmi, G. W.; Lynch, V. *Inorg. Chem.* **1993**, *32*, 3175−3187.
(39) Sessler, J. L.; Dow, W. C.; O'Connor, D.; Harriman, A.; Hemmi, G.; Mody, T. D.; Miller, R. A.; Qing, F.; Springs, S.; Woodburn, K.; Young, S. W. *J. Alloys Compounds* **1997**, *249*, 146−152.
(40) Sessler, J. L.; Mody, T. D.; Hemmi, G. W.; Lynch, V.; Young, S. W.; Miller, R. A. *J. Am. Chem. Soc.* **1993**, *115*, 10368−10369.
(41) Sessler, J. L.; Burrell, A. K.; Furuta, H.; Hemmi, G. W.; Iverson, B. L.; Král, V.; Magda, D. J.; Mody, T. D.; Shreder, K.; Smith, D.; Weghorn, S. J. In *Expanded Porphyrins. Receptors for Cationic, Anionic, and Neutral Substrates*; Fabbrizzi, L., Poggi, A., Ed.; Kluwer: Dorderecht, The Netherlands, 1994; Vol. 448, pp 391−408.
(42) Young, S. W.; Woodburn, K. W.; Wright, M.; Mody, T. D.; Fan, Q.; Sessler, J. L.; Dow, W. C.; Miller, R. A. *Photochem. Photobiol.* **1996**, *63*, 892−897.
(43) Young, S. W.; Qing, F.; Harriman, A.; Sessler, J. L.; Dow, W. C.; Mody, T. D.; Hemmi, G. W.; Hao, Y.; Miller, R. A. *Proc. Natl. Acad. Sci. U.S.A.* **1996**, *93*, 6610−6615.
(44) Young, S. W.; Sidhu, M. K.; Qing, F.; Muller, H. H.; Neuder, M.; Zanassi, G.; Mody, T. D.; Hemmi, G.; Dow, W.; Mutch, J. D.; Sessler, J. L.; Miller, R. A. *Invest. Radiol.* **1994**, *29*, 330−338.
(45) For the sake of simplicity, all metallotexaphyrins in this paper will be represented as M−Tex^{2+}, i.e., without the diacetate apical ligands.
(46) Qing, F.; Woodburn, K. W.; Young, S. W. *Int. J. Radiat. Biol. Phys.* **1997**, *39*, 256S.
(47) Pica, A.; Rosenthal, D. I.; Koprowski, C.; Schea, R.; Ruckle, J.; Tishler, R.; Larner, J. M.; Arwood, D.; Haie-Meder, C.; Young, S.; Miller, R.; Holm, M.; Engel, J.; Renschler, M. F. *Int. J. Radiat. Oncol. Biol. Phys.* **1997**, *39*, 270S.
(48) Woodburn, K. W.; Fan, Q.; Miles, D. R.; Kessel, D.; Luo, Y.; Young, S. W. *Photochem. Photobiol.* **1997**, *65*, 410−415.
(49) Qing, F.; Woodburn, K. W.; Miller, R. A. Unpublished results.
(50) Neta, P.; Huie, R. E. *J. Phys. Chem.* **1985**, *89*, 1783−1787.
(51) Armstrong, D. A.; Schuler, R. H. *J. Phys. Chem.* **1996**, *100*, 9892−9899.
(52) Mikheev, N. B.; Kamenskaya, A. N. *Coord. Chem. Rev.* **1991**, *109*, 1−59.
(53) The redox potential of Gd−Tex^{2+} was recorded previously in aqueous media ($E_{1/2}$ = 0.08 V vs NHE); see ref 43.
(54) Henglein, A.; Schnabel, W.; Wendenburg, J. *Einfuhrung in die Strahlenchemie*; Verlag Chemie: Weinheim, Germany, 1969.
(55) Baral, S.; Hambright, P.; Neta, P. *J. Phys. Chem.* **1984**, *88*, 1595−1600.
(56) Richoux, M.-C.; Neta, P.; Harriman, A.; Baral, S.; Hambright, P. *J. Phys. Chem.* **1986**, *90*, 2462−2468.
(57) Guldi, D. M.; Neta, P.; Vogel, E. *J. Phys. Chem.* **1996**, *100*, 4097−4103.
(58) Guldi, D. M.; Field, J.; Grodkowski, J.; Neta, P.; Vogel, E. *J. Phys. Chem.* **1996**, *100*, 13609−13614.
(59) Guldi, D. M.; Neta, P.; Heger, A.; Vogel, E.; Sessler, J. L. *J. Phys. Chem.* **1998**, *102*, 960−967.
(60) Morehouse, K.; Neta, P. *J. Phys. Chem.* **1984**, *88*, 1575−1579.
(61) Buxton, G. V.; Greenstock, C. L.; Helman, W. P.; Ross, A. B. *J. Phys. Chem. Ref. Data* **1988**, *17*, 513−886.
(62) Neta, P. *J. Phys. Chem.* **1981**, *85*, 3678−3684.
(63) Jolly, W. L. *Ionic Radii*; McGraw-Hill: San Francisco, 1984; Appendix F, pp 550−555.
(64) One apparent deviation from this trend involves Y−Tex^{2+}. While ostensibly the Y(III) cation is similar in size to Yb(III), uncertainties in terms of coordination sphere and specific structure, preclude a direct comparison between Y−Tex^{2+} and Yb−Tex^{2+}, Lu−Tex^{2+}, etc.